



ELSEVIER

Journal of Nuclear Materials 290–293 (2001) 1059–1063

**Journal of
nuclear
materials**

www.elsevier.nl/locate/jnucmat

Study of brittle destruction and erosion mechanisms of carbon-based materials during plasma instabilities

T. Burtseva^{a,*}, A. Hassanein^b, I. Ovchinnikov^a, V. Titov^a^a STC SINTEZ D.V., Efremov Institute of Electrophysical Apparatus, 189 631, St. Petersburg 196641, Russian Federation^b Argonne National Laboratory, Argonne, IL 60439, USA

Abstract

Erosion damage due to plasma instabilities such as hard disruptions, edge-localized modes, and vertical displacement events remains a major obstacle to successful realization of the tokamak-reactor concept. As a result of these plasma instabilities, intense plasma energy that is deposited during short periods can cause severe erosion, structural damage, and surface modifications of the plasma-facing materials. Experimental work is being carried out at the high-power VIKA-93 plasma-gun facility in the Efremov Institute, Russia. Interesting results were obtained during preliminary heating of the samples (to 1200°C) and use of maximum plasma gun parameters, i.e., $E_{in} = 30 \text{ MJ/m}^2$, $\tau = 360 \mu\text{s}$. In all samples, a large increase in weight loss (up to 80%) was observed during plasma bombardment when preheating was used. Scanning electron microscope investigations have demonstrated a considerable evolution of surface recrystallization processes, especially for preheated CFC materials. Significant differences among various carbon materials are found for specimens with and without preliminary heating. © 2001 Elsevier Science B.V. All rights reserved.

Keywords: Divertor; Erosion; Carbon-based materials; Disruption; Brittle destruction

1. Introduction

Carbon-based materials such as high-thermal-conductivity doped graphites and carbon-carbon (C-C) fiber composites (with and without dopants) are the prime candidate materials, along with tungsten and beryllium, for plasma facing components (divertor plates, limiters, etc.) in future fusion devices. Because of their excellent thermal conductivities, good mechanical properties, and better plasma compatibilities these materials have been used successfully in most current tokamaks and stellarators.

Strong chemical erosion (at 600–750°C) and radiation-enhanced sublimation ($\geq 1200^\circ\text{C}$) of carbon-based materials occur during normal plasma operation regimes, as does thermal erosion during plasma instabil-

ities such as hard disruptions, edge-localized modes, and vertical displacement events. Plasma instabilities are a major obstacle to successful realization of the tokamak-reactor concept. As a result of these instabilities, the intense plasma energy that is deposited during short periods can cause severe erosion, structural damage, and surface modifications of plasma-facing materials.

To significantly mitigate such destruction of plasma-facing materials, recrystallized graphites and C-C fiber composites with various dopants such as carbides of titanium, silicon, or boron were developed. The C-C composites, as materials for high-heat-flux components, have demonstrated excellent resistance to thermal fatigue and thermal shock under cyclic and off-normal transient heat loads.

The aim of this study was to investigate in detail the erosion and damage mechanisms of carbon-based materials during plasma instabilities, as well as to understand the influence of various doped elements on the erosion resistance of carbon materials.

* Corresponding author. Tel.: +7-812 462 7643; fax: +7-812 464 4623.

E-mail address: burts@sintez.niiefa.spb.su (T. Burtseva).

2. Disruption simulation experiments

2.1. Experiments in plasma accelerator VIKA

During the last several years, plasma disruption simulation experiments were carried out in the VIKA-series plasma accelerators (VIKA, VIKA-92, and VIKA-93) at the D.V. Efremov Institute, Russia [1–3].

VIKA is a coaxial plasma gun that can deliver intense plasma pulses with durations of 30–360 μs . The maximum electrical energy that can be stored in the capacitor banks is $E_{\text{el}} = 100$ kJ at a voltage of $U_{\text{max}} = 5$ kV. The parameters of the plasma flow and plasma/target interaction processes were investigated by using complex and sophisticated diagnostic measures. Diagnostics included spectroscopic devices for observing plasma radiation over a wide spectral range (from far ultraviolet to visible wavelengths), laser interferometry, high-speed photo-recorder, and devices for plasma pulse and energy measurements (integral calorimeter and ballistic pendulum). Spectroscopy measurements of the electron temperature, T_e , in experiments during the interaction of plasma flow with various target materials showed values of $T_e \approx 7\text{--}9$ eV at 1–2 mm above the target. The target plasma density in VIKA-92 experiments exceeded $1\text{--}2 \times 10^{24}$ m^{-3} (measurements of He–Ne-laser radiation absorption), while for the VIKA-93 experiments, the density was $>3\text{--}5 \times 10^{23}$ m^{-3} . The accelerated plasma flow is characterized by a velocity of 0.4–1.7 m/s. In all of these experiments, the specimens were exposed to plasma pulses with normal incidence at the specimen surfaces.

The first results from the VIKA facility and from the electron beam accelerator [2] were similar. This conclusion was reached by comparing the weight loss data for thermal erosion. Microscopic studies have also revealed general patterns in the changes of surface morphology.

2.2. Investigated regimes and materials

A new series of experiments on various carbon-based materials was carried out at the modernized pure-plasma accelerator VIKA-93 in the 360 μs regime with and without preliminary heating (1200°C) at fixed values of 30 MJ/m^2 incident energy. These parameters provide the highest weight losses in the graphite targets. Samples measuring $\sim 25 \times 25 \times 10$ mm^3 were placed in the EK-98 graphite sample holder, allowing the edge effect to be neglected during testing. Therefore, the total sample surface was the effective area of impact.

Surface damage and material erosion were investigated for the following different carbon-based materials:

1. Recrystallized graphites: RG-Ti-91 (7.5 wt% Ti), RG-Ti-Si (7.5 wt% Ti, 2.5 wt% Si), and RG-Ti-B (7.5 wt% Ti, 0.1 wt% B).
2. Fine-grain graphite: POCO-AXF-5Q.

3. Carbon-fiber composites (CFC):

- 3.1. UAM-92-5D (PAN fibers, $1.5 \times 1.5 \times 0.75$ mm).
- 3.2. UAM-93-5D-B (PAN fibers, $2 \times 2 \times 1.5$ mm, ≈ 1 wt% B).
- 3.3. UAM-93-5D-Ti (PAN fibers, $3 \times 3 \times 1.5$ mm, 1 wt% Ti).
- 3.4. CXB-400L (with boron, ~ 10 wt%).
- 3.5. CX-30002U (felt).

Before and after plasma exposure, the sample weight was measured, the surface morphology was examined by scanning electron microscopy (SEM), and the distribution of doped elements was analyzed by X-ray microanalyses (XMA).

3. Results

3.1. Behavior of CFC materials

Significant differences among the carbon materials were found in specimens with and without preliminary heating. The weight losses per shot are shown in Fig. 1. In all samples, a large increase in weight loss (up to 80%) was observed during plasma bombardment after preheating. The least weight loss was seen in the CX-30002U felt composite. RG-Ti-91 recrystallized graphite confirmed its good erosion resistance under various radiation fluxes. There was no significant effect of minimal (0.1%) boron and Ti doping on the amount of eroded materials. Maximum thermal erosion was seen in the boron-containing Japanese C–C composite CXB-400L.

SEM investigation demonstrated a considerable evolution of surface recrystallization processes, especially for preheated CFC materials. Surface modification with intensive formation of high porosity and cracks in all C–C composites with and without doping are shown in Fig. 2. The primary observation from surface microstructure is that all of the CFC composites eroded in a similar and very uniform manner. Cracking of C–C fiber composites usually occurs in the direction parallel to the fibers (see Fig. 3) and cracking of fibers occurs only occasionally (also, recrystallization processes can be partially responsible for crack formation; see Fig. 4).

UAM-type composites displayed numerous spherical formations, seen as blisters (Fig. 5(a)). However, in Fig. 5(b) it is possible to see the destruction of these formations. From detailed analysis, it was shown that these formations, as well as fiber destruction, are the result of enhanced recrystallization processes at graphite surfaces during intensive plasma irradiation combined with high-temperature heating.

Carbon-based materials are (on a microscopic scale) rather non-uniform, with grains having a range of sizes typically from 1 to 200 μm . During intensive heating, thermal stresses develop and lead to the disintegration of

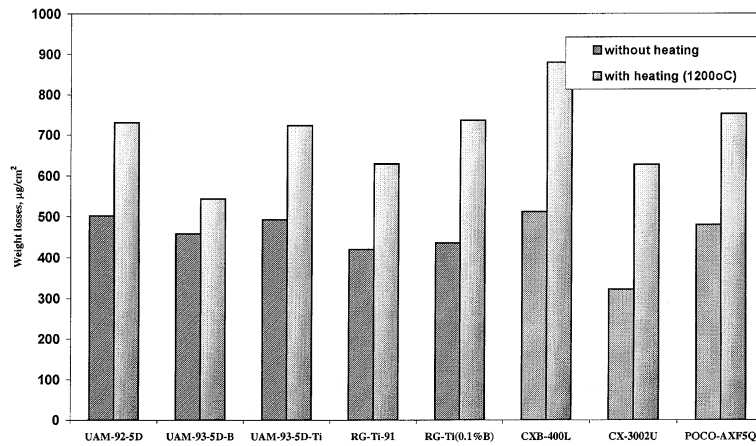


Fig. 1. Thermal erosion of various carbon-based materials after plasma irradiation at VIKA facility with and without preheating ($E_{inc} = 30 \text{ MJ/m}^2$, $\tau_{pulse} = 360 \text{ }\mu\text{s}$, $T_{preheat} = 1200^\circ\text{C}$).

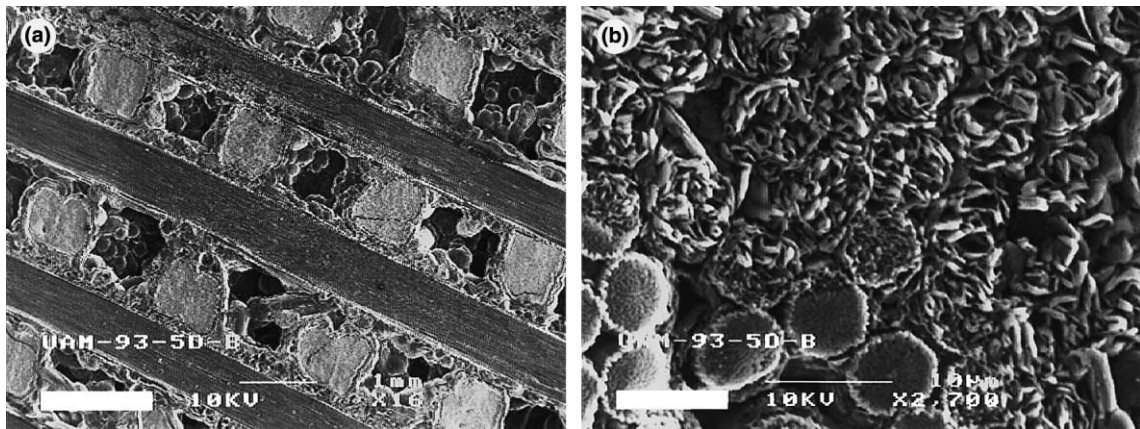


Fig. 2. Surface modification and pore formation in UAM-93-5D-B carbon composite during plasma irradiation at VIKA facility ($E_{inc} = 30 \text{ MJ/m}^2$, $\tau_{pulse} = 360 \text{ }\mu\text{s}$, $T_{preheat} = 1200^\circ\text{C}$).

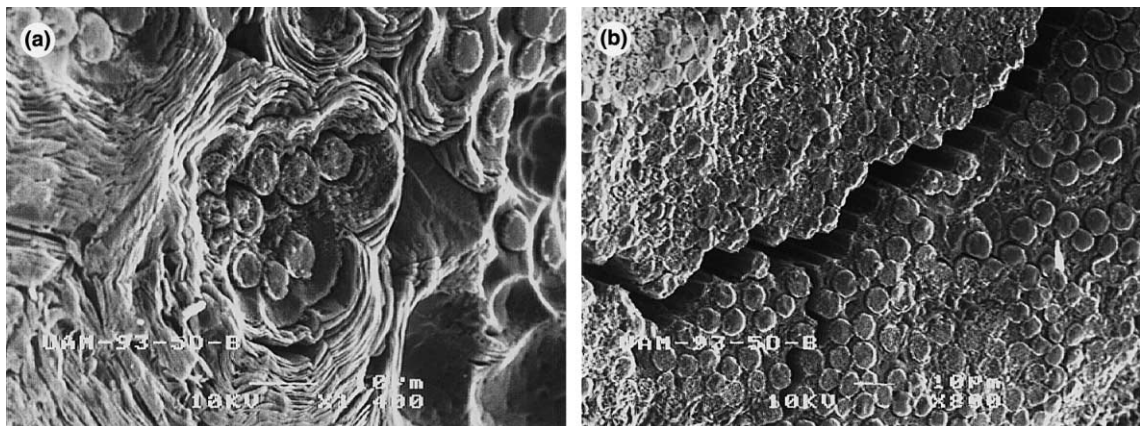


Fig. 3. (a) Surface modification and (b) crack formation of UAM-type carbon composites during plasma irradiation.



Fig. 4. Surface recrystallization and new structure formation for CFC materials during plasma irradiation.

single grains, resulting in enhanced erosion [4]. This is more pronounced in low-density graphites and C–C composites, which have generally coarser grains. Also, single grains may become overheated due to poor contact with their neighbors, leading to localized sublimation, brittle destruction, extensive recrystallization processes, and therefore higher erosion.

Enrichment (up to two or three times) by boron carbide was found on some surface layers of UAM-93-5D-B composite. As an opposite case after plasma bombardment, no noticeable titanium carbide was detected near the surface layer of CFC titanium-doped material UAM-92-5D-Ti, nor was boron carbide seen in the CXB-400L composite. The dopants were sublimated from these materials under high heat fluxes after the first plasma pulse.

This result confirms our previous electron-beam and plasma disruption simulation tests [2,3], as well as the

tests and conclusions of other studies [5,6]. Various CFC composite types with varied fiber architecture, degree of fiber/matrix constituent combinations, dopants and methods of their introduction into the base material, and technological process parameters (final graphitization temperature etc.) have a very strong influence on the quality of the composites and their resistance to high heat fluxes. The behavior of two C–C composites (Russian Ti-doped and Japanese B-doped) is a good example. When the final structures were not formed in both cases during the manufacturing process, the materials had very weak bonding between matrix, fiber, and dopes and as a result had the lowest thermal conductivity, very high porosity, high crack formation and high thermal erosion.

3.2. Behavior of doped recrystallized graphites

New small-size ($\sim 1\text{--}10\ \mu\text{m}$) titanium carbide and boron carbide formations were found on the surface of doped recrystallized graphite and were significantly enriched by doped components (for example: up to 30–50 wt% by TiC; see Fig. 6). From SEM investigations, we can conclude that brittle destruction also occurs in RG-Ti-type graphite. However, because of the more perfect structure of recrystallized graphite and the more stable bonds between grains, the consequences of brittle destruction are not so destructive as for CFC materials.

It was also noted that, after plasma bombardment, no noticeable Si was detected near the surface layers of a CFC and graphite doped with silicon carbide. This confirms our previous disruption experiments at the e-beam facility [2], in which silicon was also removed from the carbon structures at relatively low temperatures ($\leq 1600^\circ\text{C}$).

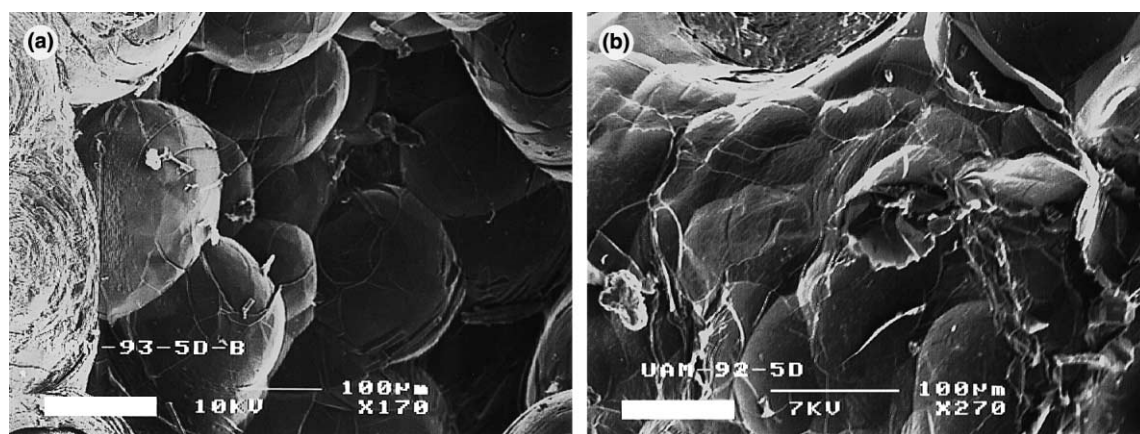


Fig. 5. (a) Spheroid formation on surface of CFC materials and (b) destruction during plasma irradiation ($E_{\text{inc}} = 30\ \text{MJ/m}^2$, $\tau_{\text{pulse}} = 360\ \mu\text{s}$, $T_{\text{preheat}} = 1200^\circ\text{C}$).

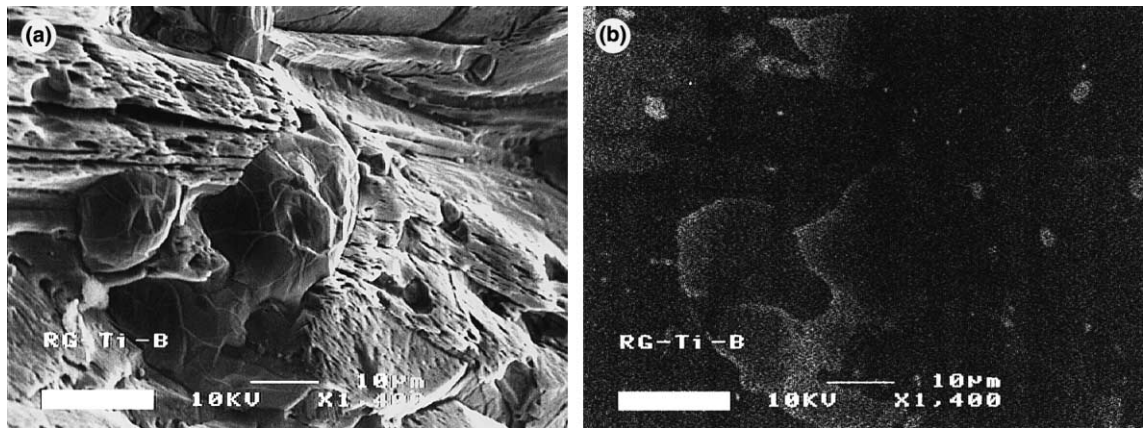


Fig. 6. (a) Surface modification, cracks and pore formations in RG–Ti–B recrystallized graphite during plasma irradiation ($E_{\text{inc}} = 30 \text{ MJ/m}^2$, $\tau_{\text{pulse}} = 360 \mu\text{s}$, $T_{\text{preheat}} = 1200^\circ\text{C}$); (b) distribution of doped elements.

4. Conclusions

This study of the behavior of various carbon-based materials under heavy thermal load has shown that brittle destruction could be a serious problem for carbon materials as candidate for plasma-facing components. Graphite materials are very non-uniform materials and are thus subject to high erosion and crack formation. During intense heating of graphite structures, the single grains become overheated due to poor contact with their neighbors, leading to localized sublimation, brittle destruction, extensive recrystallization processes, and thus higher erosion. To gain a better understanding of these processes, it is necessary to continue studying the effect of high heat loads on various graphite structures and to develop new carbon-based materials with different dopants and more perfect and improved structures at the microscopic level.

Acknowledgements

This work is partially supported by the Russian Ministry of Science, and partially by the US Department of Energy (Office of Fusion Energy Science) under contract W-31-109-Eng-38.

References

- [1] V. Barabash et al., *Fus. Eng. Des.* 18 (1991) 145.
- [2] T. Burtseva et al., *J. Nucl. Mater.* 191–194 (1992) 309.
- [3] T. Burtseva et al., *Fus. Technol.* 1 (1994) 235.
- [4] A. Hassanein, I. Konkashbaev, *J. Nucl. Mater.* 273 (1999) 326.
- [5] V. Engelko et al., *Fus. Technol.* 1 (1994).
- [6] P.G. Valentine et al., *J. Nucl. Mater.* 233–237 (1996) 660.